Available online at www.sciencedirect.com
SCIENCE DIRECT®
Journal of Magnetic Resonance 173 (2005) 317–321
JMR Journal of Magnetic Resonance
www.elsevier.com/locate/jmr

Communication

Fast multidimensional NMR: radial sampling of evolution space

Eriks Kupče, Ray Freeman*

Varian, Ltd, Eynsham, Oxford, UK
Jesus College, Cambridge University, Cambridge CB5 8BL, UK

Received 8 November 2004; revised 10 December 2004
Available online 22 January 2005

Abstract

Multidimensional NMR spectroscopy can be speeded up by limited radial sampling of the time-domain evolution data. The resulting frequency-domain projections are used to reconstruct the full NMR spectrum. New algorithms are proposed to suppress back-projection artifacts while retaining optimum sensitivity. The method is illustrated by experiments on the 900 MHz HNCO spectrum of a protein, HasA.

Keywords: Multidimensional NMR; Projection–reconstruction; Radial sampling; Artifacts; HasA

1. Introduction

Increases in magnetic field strength and dimensionality of NMR experiments have provided powerful new tools for investigating proteins [1,2]. Unfortunately this comes at the cost of dramatically prolonged measurement times. Recent attempts to tackle this problem by using highly truncated data sets [3,4] or nonlinear sampling [5,6] are based on predicting the missing data points by fitting the time-domain data to an assumed model signal. This is usually an effort- and time-consuming procedure because nothing is known about the multidimensional spectrum a priori, so it has to be guessed. The Fourier transform of such incompletely sampled data is either seriously corrupted or provides too little information for conventional analysis.

Recently, we have proposed a different strategy—radial sampling of the time-domain data in evolution space by linking the indirect time variables together in suitable proportions. Although this is another example of sparse data sampling, in this case the Fourier transform provides an excellent starting point for deriving the multidimensional spectrum. If the time-domain data set is sampled by a section inclined at an angle α, the Fourier transform is a projection onto a plane inclined at the same angle α in the frequency domain [7,8]. This method generates a set of plane projections that can be used to reconstruct the full spectrum [9,10]. The concept is analogous to established schemes employed in X-ray tomography [11] and magnetic resonance imaging [12]. The resulting speed advantage depends on the complexity of the spectrum and can be as high as an order of magnitude for each new frequency dimension beyond two, opening the door to an exciting range of higher-dimensional measurements or the investigation of time-sensitive phenomena.

The projection–reconstruction method enjoys the same sensitivity advantage per unit time as classical multidimensional spectroscopy because all the time-domain signals contribute to the final spectrum. Hence it works in situations of marginal sensitivity where other ''reduced dimensionality'' approaches can experience difficulties. However, it is important to choose reconstruction schemes that preserve this signal-to-noise advantage. This is not the case for the ''lower-value

* Corresponding author. Fax: +44 1223 336362.
E-mail address: rf110@hermes.cam.ac.uk (R. Freeman).

1090-7807/$ - see front matter © 2004 Elsevier Inc. All rights reserved.
doi:10.1016/j.jmr.2004.12.004

algorithm'' (outlined below) which was conceived for samples of good intrinsic sensitivity. It is also important to avoid the introduction of artifacts into the reconstructed spectrum, as often happens with back-projection schemes based on the inverse Radon transform, particularly if only a few projections are used [13,14].

1.1. Reconstruction algorithms

Consider, for the sake of illustration, a three-dimensional experiment, although the procedure is readily extended to higher dimensions. The data array $F_1F_2F_3$ is built up one F_1F_2 plane at a time. There are several possible modes of attack. A method that has already been employed [9,10] starts with the measured one-dimensional projections on the F_1 and F_2 axes. Cross-peak in the F_1F_2 plane are predicted by scaling the F_1 traces according to the intensities in the F_2 trace (or vice versa). This generates a ''provisional'' spectrum where the frequencies are correct but the intensities are under-determined. The latter are corrected by using information from tilted projections, achieved very effectively by employing the ''lower-value'' algorithm [15,16]. Unfortunately these additional projections do nothing to improve the signal-to-noise ratio, although the noise is slightly reduced in empty regions of the spectrum where there is no advantage to be gained. This is clearly an inefficient use of spectrometer time; it would be preferable if all the measurements contributed to the overall sensitivity.

The preferred scheme invokes a method related to the inverse Radon transform [13,14]. Projections are recorded at a small number of different values of α. Each one is extended at right angles to form a set of parallel ridges running across the F_1F_2 plane at an angle $(90° - \alpha)$. These ''back-projections'' are summed so that intensity builds up linearly at locations where they reinforce, generating genuine cross-peaks with essentially optimum signal-to-noise ratio. However, the method involves two kinds of artifacts—weak residual ridges that criss-cross the F_1F_2 plane and false peaks where some (but not all) of the relevant ridges intersect. The larger the number N of independent projections, the weaker the artifacts in comparison with genuine cross-peaks, but unfortunately the experimental duration increases with N. The present communication suggests two procedures for suppressing such artifacts so that a clean multidimensional spectrum can be constructed from the smallest number of projections.

1.2. Iterative extraction of cross-peaks

This scheme is loosely related to a method employed in radioastronomy [17,18] and later adapted for NMR spectroscopy to generate pure-phase spectra, eliminate truncation artifacts [19], or enhance resolution [20]. In radioastronomy interferometry, a regularly spaced two-dimensional array of detectors is employed. In practice this equipment can generate undesirable side-lobe patterns due to malfunctioning elements or occultation by the moon, together with artifacts known as grating responses due to coarse coverage. The data-processing scheme introduced by Högbom [18] cleans up the experimental star map by progressively subtracting the intensity of the strongest response (along with its associated artifacts) until all ''dirty'' responses significantly above the noise floor have been removed. Since the form of the sidelobes and grating responses are known, the corresponding ''clean'' signals can then be reassembled to give the desired star map.

The algorithm for suppressing artifacts in a reconstructed NMR spectrum possesses some similar features, because each genuine cross-peak carries with it a known pattern of undesirable ridges. It can be confidently assumed that the tallest response in the F_1F_2 plane is a valid cross-peak rather than an artifact. A search program locates this strongest peak and subtracts its associated peaks from all the projections. The cross-peak parameters are stored, and are eventually used for the construction of the final spectrum. A new version of the F_1F_2 spectrum is then constructed from the depleted projections; it no longer contains the web of ridges from the tallest cross-peak; in the process some false peaks are also suppressed. The cycle is repeated, and once all the peaks significantly above the noise floor have been removed from the projections, the offending ridges and false cross-peaks disappear, leaving a noisy baseplane containing some very weak signals and artifacts—the ''residual spectrum.'' The genuine cross-peaks are now reintroduced into this residual spectrum, stripped of their webs of ridges. Note that no significant experimental information is destroyed in this procedure; very weak responses comparable with the noise are all retained but they are unlikely to be accompanied by any noticeable ridges or false peaks.

1.3. Algebraic algorithm

Each NMR response in one of the projections defines a line [10] running across the F_1F_2 plane at an angle $(90° - \alpha)$. A genuine cross-peak occurs when lines from *every* projection (one from each) all intersect at the same point in this plane. When experimental errors are taken into account, to ''intersect'' means to fall within a small area defined by the experimental errors in the frequencies. In contrast, false cross-peaks always involve fewer intersections, sometimes only two. Consequently, the solutions of the corresponding sets of linear equations define the locations of the true cross-peaks.

Suppose there are k projections at various inclinations α_1 through α_k. Each projection is broken down into a set of n individual responses by a line-fitting procedure

that yields the frequency F_n, its intensity I_n, and full linewidth Δ_n. This search is terminated just before the noise threshold is reached. The correlation stage operates with the frequencies F_n together with an estimate for the digitization errors for that particular projection. Starting with a frequency from the first chosen projection and the known value of $(90° - \alpha)$ an equation is written for the first skew diagonal. Similar equations are written for one frequency selected from each of the remaining projections. These k simultaneous equations are examined in pairs to establish the intersection points. If all the intersections coincide within the acceptable frequency errors, this defines the location of a genuine cross-peak. (Other identifying criteria include the intensities and linewidths, and the associated F_3 frequencies.) These frequencies are then disregarded while the iteration examines the remaining simultaneous equations, continuing until all pairwise combinations have been tested. As in the previous algorithm, the genuine cross-peaks are then reintroduced into the residual spectrum.

The iterative extraction algorithm has been applied to the projection–reconstruction of the 900 MHz constant-time HNCO spectrum of a 1.7 mM aqueous solution (10% D_2O) of the isotopically enriched 187-residue protein HasA. The orthogonal NH and CH planes used 128 complex data points, and required 20 min of data acquisition each. To obtain better sensitivity and lineshape, the NH plane was actually borrowed from a two-dimensional HSQC experiment. Projections of the three-dimensional HNCO spectrum were recorded for $\alpha = \pm 60°$, using 100 complex data points, requiring 30 min. For the purposes of illustration a typical F_1F_2 plane corresponding to a proton frequency of 9.184 ppm is shown as a contour plot in Fig. 1 and as a stacked-trace plot in Fig. 2. Initially, since only four projections were used, the spectrum is dominated by prominent ridges and false peaks. The search program locates the three tallest cross-peaks in the F_1F_2 plane and stores their parameters in a separate location. The corresponding responses are subtracted (one at a time) from the F_1 and F_2 projections, progressively simplifying the new back-projections. The final back-projection of the depleted F_1 and F_2 traces creates a residual spectrum, a virtually ''blank canvas'' onto which the genuine cross-peaks are reintroduced. This display (Figs. 1D and 2D) comprises three clearly defined C–N correlation

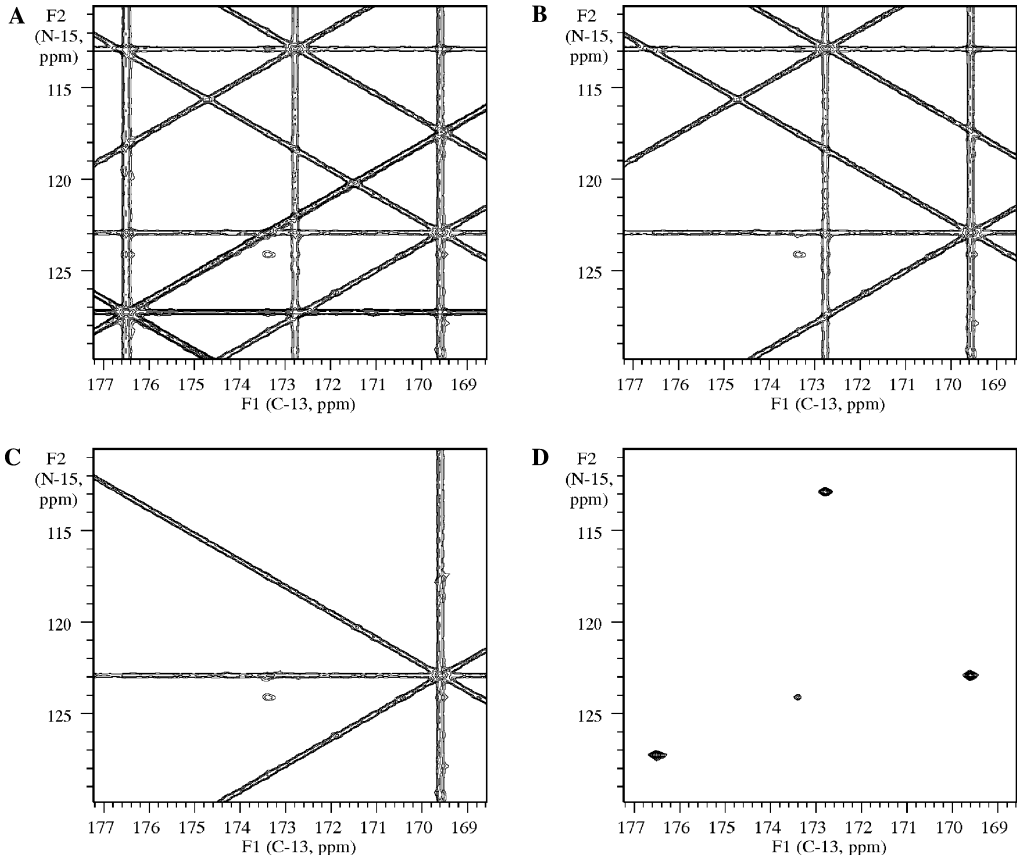

Fig. 1. C–N correlations in one plane of the three-dimensional HNCO spectrum of the HasA protein, obtained by back-projection and shown as contour plots. (A) Initially the ridges and false peaks complicate the display. (B) After peaks from one cross-peak were removed from the F_1 and F_2 projections. (C) After peaks from two cross-peaks were removed. (D) After peaks from three cross-peaks were removed; the genuine cross-peaks were then reintroduced into the residual spectrum.

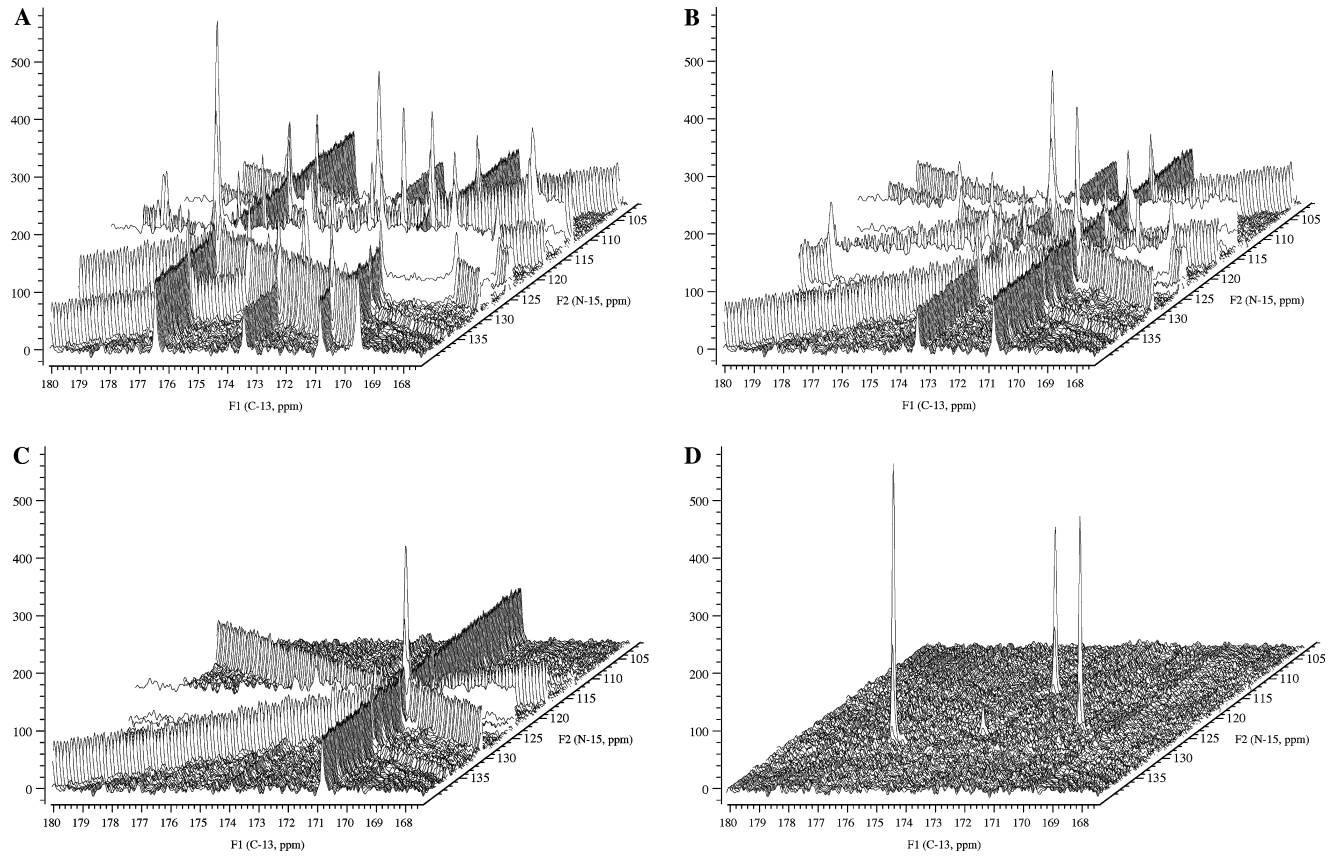

Fig. 2. As Fig. 1, but displayed as stacked traces, emphasizing the relative intensities.

peaks. The very weak tail of a signal from a nearby plane serves to emphasize the high sensitivity.

The goal of the additive algorithm is to improve the signal-to-noise ratio of the reconstructed spectra in comparison with the earlier "lower-value" algorithm. Although the latter is very effective in eliminating artifacts, the signal-to-noise ratio is determined, once and for all, when the two orthogonal projections have been processed; it does not improve as additional projections are included. By contrast, the additive algorithm treats all N projections even-handedly, and boosts the signal-to-noise ratio as the square root of N, as in conventional multiscan averaging. The disadvantage of back-projection is the presence of artifacts, but the proposed iterative extraction scheme reduces these by a very large factor. Fig. 2, recorded for the worst-possible case of only four projection angles, demonstrates a 40-fold suppression of the most prominent artifact.

There are those who would argue that the numerical results of this operation (frequencies, intensities, and correlations) are all that is needed for sequencing the aminoacid residues of a protein, particularly when an automated program is used. We believe this to be a short-sighted view. Reconstruction of the actual multidimensional spectrum is important. It is the best way to assess the reliability of the experimental data, and it translates any errors in the reconstruction algorithm into artifacts, such as webs of ridges that would normally have been eliminated. The spectrum also brings to light weak peaks that may be overlooked by a purely numerical analysis. It would be a great mistake to belittle the importance of real spectra.

Acknowledgments

The authors are indebted to Dr. Anne Lecroisey and Dr. Muriel Delepierre of the Institute Pasteur for the protein sample HasA, to Professor Yoshifumi Nishimura of Yokohama City University for permission to use the 900 MHz spectrometer, and to Dr. Junichi Kurita of Varian for help in setting up the experiments.

References

[1] M. Saltzmann, K. Pervushin, G. Wider, H. Senn, K. Wüthrich, NMR assignment and secondary structure determination of an octameric 110 kDa protein using TROSY in triple resonance experiments, J. Am. Chem. Soc. 122 (2000) 7543–7548.

[2] V. Tugarinov, R. Muhandiram, A. Ayed, L.E. Kay, Four-dimensional NMR spectroscopy of a 723-residue protein:

chemical shift assignments and secondary structure of malate synthetase G, J. Am. Chem. Soc. 124 (2002) 10025–10035.
[3] J. Chen, V.A. Mandelshtam, A.J. Shaka, Regularization of the two-dimensional filter diagonalization method: FDM2K, J. Magn. Reson. 146 (2000) 363–368.
[4] J. Chen, A.A. De Angelis, V.A. Mandelshtam, A.J. Shaka, Progress on the two-dimensional filter diagonalization method. An efficient doubling scheme for two-dimensional constant-time NMR, J. Magn. Reson. 161 (2003) 74–89.
[5] V.Y. Orekhov, I.V. Ibraghimov, M. Billeter, MUNIN: a new approach to multidimensional NMR spectra interpretation, J. Biomol. NMR 20 (2001) 49–60.
[6] D. Rovnyak, J.C. Hoch, A.S. Stern, G. Wagner, Resolution and sensitivity of high-field nuclear magnetic resonance spectroscopy, J. Biomol. NMR 30 (2004) 1–10.
[7] R.N. Bracewell, The projection-slice theorem, Aust. J. Phys. 9 (1956) 198.
[8] K. Nagayama, P. Bachmann, K. Wüthrich, R.R. Ernst, The use of cross-sections and of projections in two-dimensional NMR spectroscopy, J. Magn. Reson. 31 (1978) 133.
[9] E. Kupče, R. Freeman, Reconstruction of the three-dimensional NMR spectrum of a protein from a set of plane projections, J. Biomol. NMR 27 (2003) 383–387.
[10] E. Kupče, R. Freeman, The projection–reconstruction technique for speeding up multidimensional NMR spectroscopy, J. Am. Chem. Soc. 126 (2004) 6429–6440.
[11] G.N. Hounsfield, Computerized transverse axial tomography, Br. J. Radiol. 46 (1973) 1016.
[12] P.C. Lauterbur, Image formation by induced local interactions: examples employing nuclear magnetic resonance, Nature London 242 (1973) 190–191.
[13] S.R. Deans, The Radon Transform and Some of its Applications, Wiley, New York, 1983.
[14] E. Kupče, R. Freeman, The radon transform: a new scheme for fast multidimensional NMR, Concept. Magnetic Res. A 22 (2004) 4–11.
[15] R. Baumann, G. Wider, R.R. Ernst, K. Wüthrich, Improvement of 2D NOE and 2D correlated spectra by symmetrization, J. Magn. Reson. 44 (1981) 402.
[16] L. McIntyre, X.-L. Wu, R. Freeman, Fine structure of cross-peaks in truncated COSY experiments, J. Magn. Reson. 87 (1990) 194–201.
[17] J.G. Ables, Maximum entropy spectra analysis, Astron. Astrophys. Suppl. 15 (1974) 383.
[18] J.A. Högbom, Aperture synthesis with a non-regular distribution of interferometric baselines, Astron. Astrophys. Suppl. 15 (1974) 417.
[19] A.J. Shaka, J. Keeler, R. Freeman, Separation of chemical shifts and spin coupling in proton NMR. Elimination of dispersion signals from two-dimensional J-spectra, J. Magn. Reson. 56 (1984) 294–313.
[20] S.J. Davies, C. Bauer, P.J. Hore, R. Freeman, Resolution enhancement by non-linear data processing. "HOGWASH" and the maximum entropy method, J. Magn. Reson. 76 (1988) 476–493.